

CONTRIBUTION FROM BELL LABORATORIES, MURRAY HILL, NEW JERSEY 07974,
AND THE DEPARTMENT OF INORGANIC CHEMISTRY, UNIVERSITY OF MELBOURNE, PARKVILLE, 3052 AUSTRALIA**Magnetic Exchange in Transition Metal Complexes. IX.^{1a}**
Dimeric Nickel(II)-Ethylenediamine ComplexesBY A. P. GINSBERG,*^{1b} R. L. MARTIN,^{1c} R. W. BROOKES,^{1c} AND R. C. SHERWOOD^{1b}

Received April 18, 1972

The magnetic susceptibility of the dimeric complexes $[\text{Ni}_2(\text{NH}_2\text{CH}_2\text{CH}_2\text{NH}_2)_4\text{X}_2]\text{Y}_2$ ($\text{X}, \text{Y} = \text{Cl}, \text{Br}; \text{X} = \text{NCS}, \text{Y} = \text{I}$) has been determined as a function of temperature in the range 1.5–300°K and as a function of field from 1 to 15.3 kOe. The results are interpreted on the basis of an isotropic intradimer exchange Hamiltonian with the inclusion of single-ion zero-field splitting and interdimer exchange in the molecular field approximation. Intradimer parallel spin coupling ($S = 2$ ground state) is found in all three compounds; the exchange integrals are $J(\text{X} = \text{Cl}) \approx 10 \text{ cm}^{-1}$, $J(\text{X} = \text{Br}) \approx 8 \text{ cm}^{-1}$, and $J(\text{X} = \text{NCS}) \approx 5 \text{ cm}^{-1}$. The intradimer coupling in the thiocyanate complex is the first example of ferromagnetic exchange *via* a polyatomic bridge in a cluster complex; it evidences the transmission of parallel spin coupling through multi-center molecular orbitals.

Introduction

Di- μ -chloro-tetrakis(ethylenediamine)dinickel(II) chloride and di- μ -bromo-tetrakis(ethylenediamine)dinickel(II)bromide are, respectively, Cl- and Br-bridged dimers with the structure² illustrated in Figure 1. The related thiocyanate complex, di- μ -thiocyanato-tetrakis(ethylenediamine)dinickel(II) iodide, has the NCS-bridged dimer structure³ shown schematically in Figure 2. We have measured the magnetic susceptibility of these compounds as a function of temperature from 300 to 1.5°K and as a function of field from 1 to 15.3 kOe. The results demonstrate that the *intra*-molecular exchange coupling in the three compounds is ferromagnetic (spins in the molecular ground state aligned parallel, exchange integral J positive) with similar exchange integrals. This is a significant conclusion in two respects. In the first place $[\text{Ni}_2(\text{en})_4(\text{SCN})_2]\text{I}_2$ represents the first example, in a cluster complex, of ferromagnetic exchange coupling between metal atoms linked by polynuclear bridges;⁴ all other examples of this phenomenon, *e.g.*, $\text{Ni}_3(\text{acac})_6$ ⁵ or $\text{Ni}_4(\text{OCH}_3)_4(\text{acac})_4(\text{CH}_3\text{OH})_4$,⁶ involve monatomic bridges between the metal atoms, as in $[\text{Ni}_2(\text{en})_4\text{X}_2]\text{X}_2$ ($\text{X} = \text{Cl}, \text{Br}$). In the second place the occurrence of exchange coupling with the same order of magnitude in both $[\text{Ni}_2(\text{en})_4\text{X}_2]\text{X}_2$ and $[\text{Ni}_2(\text{en})_4(\text{SCN})_2]\text{I}_2$, in spite of the great difference in Ni–Ni distance (5.8 Å in the thiocyanate complex and probably about 3.5 Å in the chloride complex), demonstrates the relative unimportance of the metal–metal distance in determining the strength of exchange interactions, so long as there exist appropriate pathways for exchange coupling through bridging ligands.

Theory

The nickel dimers contain "octahedrally" coordinated divalent nickel. Since the single-ion ground state is an

orbital singlet, it is appropriate to use the isotropic spin-coupling Hamiltonian⁷

$$\mathcal{H}_0 = -2J\hat{s}_1 \cdot \hat{s}_2 \quad (1)$$

where J is the exchange integral for the intradimer interaction between nickel atoms with spin operators \hat{s}_1 and \hat{s}_2 . If we include the effect of an external magnetic field H along the z direction and also allow for an interdimer interaction in the molecular field approximation,^{1a} the Hamiltonian becomes

$$\mathcal{H} = -2J\hat{s}_1 \cdot \hat{s}_2 - g\beta H\hat{S}_z - 2Z'J'\hat{S}_z\langle\hat{S}_z\rangle \quad (2)$$

where \hat{S}_z is the operator for the z component of total dimer spin, J' is the effective interdimer exchange integral, and Z' is the dimer lattice coordination number.

Let s be the eigenvalues of \hat{s}_1 or \hat{s}_2 , S the eigenvalues of $\hat{s}_1 + \hat{s}_2$, and M_s the eigenvalues of \hat{S}_z . The eigenvalues of (1) are

$$E_0(S, M_s) = -J[S(S+1) - 2s(s+1)] \quad (3)$$

while those of (2) may be written

$$E(S, M_s) = E_0(S, M_s) - g\beta H M_s - 2Z'J'M_s\langle\hat{S}_z\rangle \quad (4)$$

Divalent nickel has two unpaired spins per atom, so that $s = 1$ and $S = 2, 1, 0$. The energy levels $E_0(S, M_s)$ are therefore $E_0(0, 0) = +4J$, $E_0(1, M_1) = +2J$, and $E_0(2, M_2) = -2J$, where $M_s = S, S-1, \dots, -S$ and each level is $(2S+1)$ -fold degenerate when H is zero. Proceeding as in ref 1a we obtain the susceptibility, χ_A' , per gram-atom of nickel

$$\chi_A' = \{Ng^2\beta^2 F(J, T) / [kT - 4Z'J'F(J, T)]\} + N\alpha \quad (5)$$

where

$$F(J, T) = \left[\frac{1 + 5e^{4J/kT}}{3 + 5e^{4J/kT} + e^{-2J/kT}} \right] \quad (6)$$

$N\alpha$ is a correction added to take account of the temperature-independent paramagnetism.

Figure 3a shows plots of eq 5, in the form of $\mu_{\text{eff}} = (3k(\chi_A' - N\alpha)T/N\beta^2)^{1/2}$ vs. the reduced temperature

(1) (a) Part VIII: A. P. Ginsberg and M. E. Lines, *Inorg. Chem.*, **11**, 2289 (1972). (b) Bell Laboratories. (c) University of Melbourne.

(2) A. S. Antsyshkina and M. A. Porai-Koshits, *Dokl. Akad. Nauk SSSR*, **143**, 105 (1962).

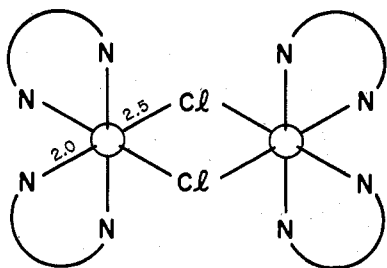
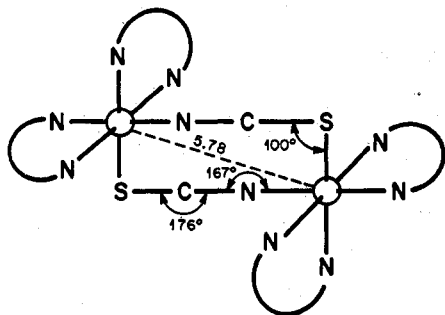
(3) A. E. Shvelashvili, M. A. Porai-Koshits, and A. S. Antsyshkina, *J. Struct. Chem. (USSR)*, **10**, 552 (1969).

(4) Preliminary communication: A. P. Ginsberg, R. C. Sherwood, R. W. Brookes, and R. L. Martin, *J. Amer. Chem. Soc.*, **93**, 5927 (1971).

(5) A. P. Ginsberg, R. L. Martin, and R. C. Sherwood, *Chem. Commun.*, 856 (1967); *Inorg. Chem.*, **7**, 932 (1968).

(6) J. A. Bertrand, A. P. Ginsberg, R. I. Kaplan, C. E. Kirkwood, R. L. Martin, and R. C. Sherwood, *ibid.*, **10**, 240 (1971).

(7) For reviews see: (a) A. P. Ginsberg, *Inorg. Chim. Acta Rev.*, **5**, 45 (1971); (b) R. L. Martin, "New Pathways in Inorganic Chemistry," E. A. V. Ebsworth, A. G. Maddock, and A. G. Sharpe, Ed., Cambridge University Press, New York, N. Y., 1968, Chapter 9.


 Figure 1.—Schematic illustration of the structure of $[\text{Ni}_2(\text{en})_4\text{Cl}_2]\text{Cl}_2$.

 Figure 2.—Schematic illustration of the structure of $[\text{Ni}_2(\text{en})_4(\text{SCN})_2]\text{I}_2$.

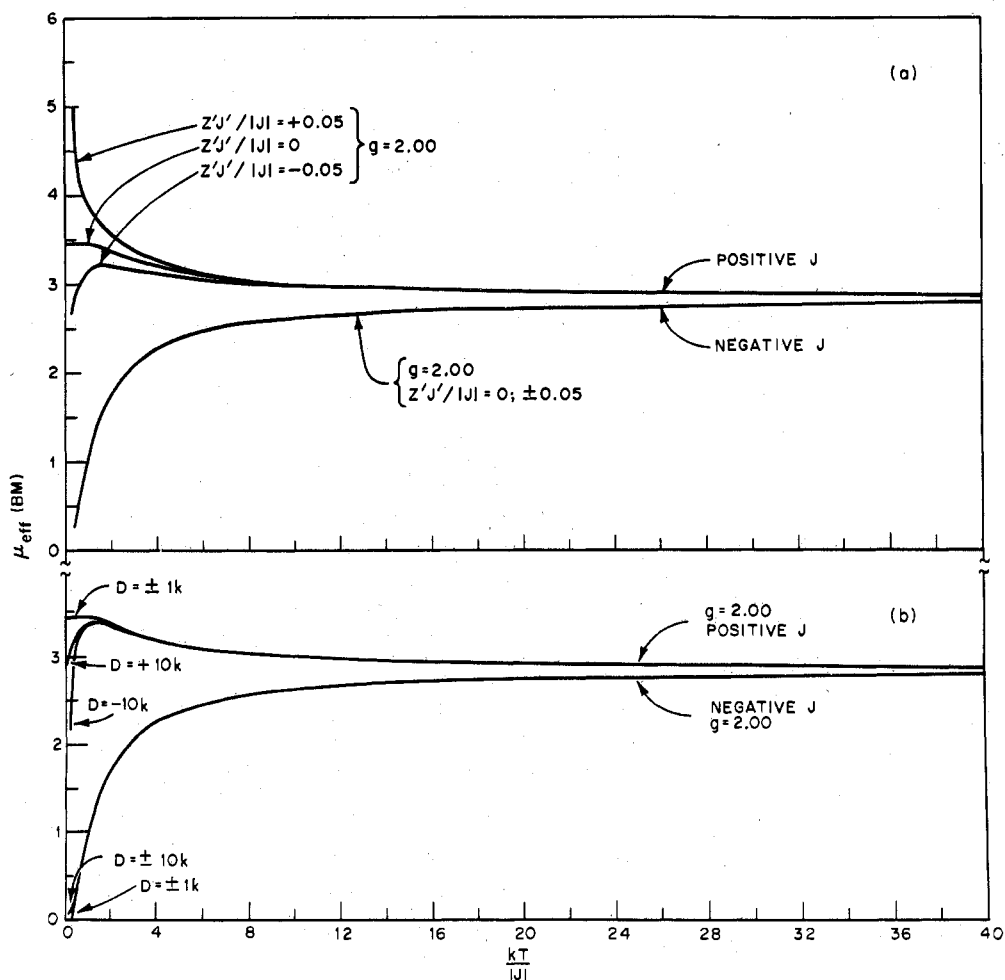
$kT/|J|$, for positive and negative J with $Z'J' = 0$ and $\pm 0.05|J|$. All of the curves have the same high-temperature limit, $\mu_{\text{eff}}(T \rightarrow \infty) = \sqrt{2}g$. When J is negative, the low-temperature limit is $\mu_{\text{eff}}(T \rightarrow 0) = 0$, and a $Z'J'$ value of $\pm 0.05|J|$ does not have a significant effect on the curve. When J is positive and the intercluster exchange is zero, the low-temperature limit is $\mu_{\text{eff}}(T \rightarrow 0) = \sqrt{3}g$. Intercluster exchange has a significant effect for positive J . Thus when $Z'J' = -0.05|J|$, the curve passes through a maximum at $kT/|J| = 1.77$, where $\mu_{\text{eff}} = 1.608g$. When $Z'J' = \pm 0.05|J|$, the curve reaches $\mu_{\text{eff}} = \sqrt{3}g$ at $kT/|J| = 2.4$; after this it continues rising, going up very rapidly below $kT/|J| = 2.0$.

Since divalent nickel can have a large zero-field splitting parameter ($D \approx 5-10k$), it is necessary to evaluate the effect of single-ion zero-field splitting on the dimer susceptibility. Let the system be quantized along the z direction and assume axial symmetry. In the absence of a magnetic field and neglecting inter-dimer interaction, the Hamiltonian is

$$\mathcal{H}_0 = -2J\hat{s}_1 \cdot \hat{s}_2 - D(\hat{s}_{1z}^2 + \hat{s}_{2z}^2) \quad (7)$$

Since $2\hat{s}_1 \cdot \hat{s}_2 = \hat{S}^2 - 2s(s+1) = \hat{S}^2 - 4$, Hamiltonian (7) may be written

$$\mathcal{H}_0 = -J\hat{S}^2 - D(\hat{s}_{1z}^2 + \hat{s}_{2z}^2) \quad (8)$$


 Figure 3.—Theoretical dependence of μ_{eff} (BM) per Ni atom upon the reduced temperature $kT/|J|$ for a dimer complex: (a) eq 5; (b) eq 19.

The basis functions ψ_s^M s in terms of the kets $|M_{s_1}, M_{s_2}\rangle$ are

$$\begin{aligned}\psi_{2^{\pm 2}} &= |\pm 1, \pm 1\rangle \\ \psi_{2^{\pm 1}} &= \frac{1}{\sqrt{2}}\{|0, \pm 1\rangle + |\pm 1, 0\rangle\} \\ \psi_{2^0} &= \frac{1}{\sqrt{6}}\{2|0, 0\rangle + |1, -1\rangle + |-1, 1\rangle\} \\ \psi_{1^{\pm 1}} &= \frac{1}{\sqrt{2}}\{|0, \pm 1\rangle - |\pm 1, 0\rangle\} \\ \psi_{1^0} &= \frac{1}{\sqrt{2}}\{|1, -1\rangle - |-1, 1\rangle\} \\ \psi_{0^0} &= \frac{1}{\sqrt{3}}\{|0, 0\rangle - |1, -1\rangle - |-1, 1\rangle\}\end{aligned}$$

\mathcal{H}_0 is easily diagonalized within this basis set to obtain the eigenfunctions $\psi_{0,n}$ and the eigenvalues $E_{0,n}$

$$\begin{aligned}\psi_{0,1} &= \psi_{2^2}; \quad \psi_{0,2} = \psi_{2^{-2}}; \quad E_{0,1} = E_{0,2} = -6J - 2D \\ \psi_{0,3} &= \psi_{2^1}; \quad \psi_{0,4} = \psi_{2^{-1}}; \quad E_{0,3} = E_{0,4} = -6J - D \\ \psi_{0,5} &= C_2\psi_{2^0} + C_1\psi_{0^0}; \quad E_{0,5} = -3J - D - \delta \\ \psi_{0,6} &= \psi_{1^1}; \quad \psi_{0,7} = \psi_{1^{-1}}; \quad E_{0,6} = E_{0,7} = -2J - D \\ \psi_{0,8} &= \psi_{1^0}; \quad E_{0,8} = -2J - 2D \\ \psi_{0,9} &= C_1\psi_{2^0} + C_2\psi_{0^0}; \quad E_{0,9} = -3J - D + \delta\end{aligned}$$

where

$$\begin{aligned}\delta &= [(3J + D)^2 - 8JD]^{1/2} \\ C_1 &= 2\sqrt{2D}/[(9J - D + 3\delta)^2 + 8D^2]^{1/2} \\ C_2 &= (9J - D + 3\delta)/[(9J - D + 3\delta)^2 + 8D^2]^{1/2}\end{aligned}$$

Let an external magnetic field H be applied along the x , y , or z direction; the Hamiltonian becomes

$$\mathcal{H} = \mathcal{H}_0 - g_i\beta H\hat{S}_i \quad (9)$$

where \mathcal{H}_0 is given by (8) and $i = x, y$, or z . When the external field is along the z direction, the eigenvalues E_n of (9) are given exactly by first-order perturbation theory since the $\psi_{0,n}$ are eigenfunctions of \hat{S}_z ; we have

$$E_n = E_{0,n} - g_z\beta H\langle\psi_{0,n}|\hat{S}_z|\psi_{0,n}\rangle \quad (10)$$

When the external field is along the x direction, the first-order perturbation energy is zero because \hat{S}_x has no diagonal elements with $\psi_{0,n}$. We must therefore calculate the second-order perturbation term. Although some of the $\psi_{0,n}$ are degenerate, there are no matrix elements of \hat{S}_x between degenerate functions; nondegenerate perturbation theory may therefore be used. The results are

$$\begin{aligned}E_1 &= E_2 = -6J - 2D - g_x^2\beta^2 H^2 D^{-1} \\ E_3 &= E_4 = -6J - D + \\ &g_x^2\beta^2 H^2 \left(D^{-1} - \frac{3C_2^2}{6J - 2\delta} - \frac{3C_1^2}{6J + 2\delta} \right) \\ E_5 &= -3J - D - \delta + \frac{3g_x^2\beta^2 H^2 C_2^2}{3J - \delta} \\ E_6 &= E_7 = -2J - D + \frac{1}{2}g_x^2\beta^2 H^2 D^{-1}\end{aligned}$$

$$E_8 = -2J - 2D - g_x^2\beta^2 H^2 D^{-1}$$

$$E_9 = -3J - D + \delta + \frac{3g_x^2\beta^2 H^2 C_1^2}{3J + \delta}$$

The susceptibility is now readily calculated by making use of the relation

$$\langle\hat{S}_i\rangle = \frac{kT}{g_i\beta} \left(\frac{\partial \ln \text{PF}}{\partial H} \right)_T \quad (11)$$

the partition function being given by

$$\text{PF} = \sum_{n=1}^9 e^{-E_n/kT} \quad (12)$$

We obtain for the field-independent susceptibilities

$$\chi_z = \frac{2Ng_x^2\beta^2}{kT} F_1(J, D, T) \quad (13)$$

and

$$\begin{aligned}\chi_x = \chi_y &= 2Ng_x^2\beta^2 \left\{ D^{-1}F_2(J, D, T) + \right. \\ &\left. \frac{3C_2^2}{3J - \delta}F_3(J, D, T) + \frac{3C_1^2}{3J + \delta}F_4(J, D, T) \right\} \quad (14)\end{aligned}$$

where

$$F_1(J, D, T) = \frac{1 + e^{4J/kT} + 4e^{4J/kT}e^{D/kT}}{2 + e^{D/kT} + e^{J/kT}e^{-\delta/kT} + e^{J/kT}e^{\delta/kT} + 2e^{4J/kT} + 2e^{4J/kT}e^{D/kT}} \quad (15)$$

$$F_2(J, D, T) = \frac{2e^{4J/kT}e^{D/kT} + e^{D/kT} - 1 - 2e^{4J/kT}}{2 + e^{D/kT} + e^{J/kT}e^{-\delta/kT} + e^{J/kT}e^{\delta/kT} + 2e^{4J/kT} + 2e^{4J/kT}e^{D/kT}} \quad (16)$$

$$F_3(J, D, T) = \frac{e^{4J/kT} - e^{J/kT}e^{\delta/kT}}{2 + e^{D/kT} + e^{J/kT}e^{-\delta/kT} + e^{J/kT}e^{\delta/kT} + 2e^{4J/kT} + 2e^{4J/kT}e^{D/kT}} \quad (17)$$

$$F_4(J, D, T) = \frac{e^{4J/kT} - e^{J/kT}e^{-\delta/kT}}{2 + e^{D/kT} + e^{J/kT}e^{-\delta/kT} + e^{J/kT}e^{\delta/kT} + 2e^{4J/kT} + 2e^{4J/kT}e^{D/kT}} \quad (18)$$

Taking $g_x = g_z = g$ (a very good approximation for Ni^{2+}) and expressing J and D in units of k , the powder susceptibility per gram-atom of Ni^{2+} is

$$\begin{aligned}\chi_A' &= \frac{Ng^2\beta^2}{3k} \left\{ \frac{F_1(J, D, T)}{T} + \frac{2}{D}F_2(J, D, T) + \right. \\ &\left. \frac{6C_2^2}{3J - \delta}F_3(J, D, T) + \frac{6C_1^2}{3J + \delta}F_4(J, D, T) \right\} + N\alpha \quad (19)\end{aligned}$$

As before, $N\alpha$ is a correction term for the temperature-independent paramagnetism.

Figure 3b shows plots of eq 19, in the form of $\mu_{\text{eff}} = (3k(\chi_A' - N\alpha)T/N\beta^2)^{1/2}$ against the reduced temperature, for positive and negative J with $D = \pm 1k$ and $\pm 10k$. In its effect on the dimer susceptibility, zero-field splitting is qualitatively similar to an antiferromagnetic interdimer interaction.

To derive a susceptibility equation including the effect of both zero-field splitting and interdimer interaction, the term $-2Z'J'\hat{S}_i\hat{S}_i$ is added to the Hamiltonian (9). Proceeding as above and in ref 1a we obtain eq 20

$$\chi_A' = \frac{Ng^2\beta^2}{3k} \left\{ \frac{F_1(J,D,T)}{T - 4Z'J'F_1(J,D,T)} + \frac{2F'(J,D,T)}{1 - 4Z'J'F'(J,D,T)} \right\} + N\alpha \quad (20)$$

where

$$F'(J,D,T) = \frac{1}{D}F_2(J,D,T) + \frac{3C_2^2}{3J - \delta}F_3(J,D,T) + \frac{3C_1^2}{3J + \delta}F_4(J,D,T) \quad (21)$$

Experimental Section

$[\text{Ni}_2(\text{en})_4\text{Cl}_2]\text{Cl}_2$ was prepared by allowing $\text{NiCl}_2 \cdot 6\text{H}_2\text{O}$ to react with $[\text{Ni}(\text{en})_3]\text{Cl}_2 \cdot 2\text{H}_2\text{O}$ in methanol containing 5% water, according to the procedure in ref 8. *Anal.* Calcd for $\text{Ni}_4\text{H}_{16}\text{N}_4\text{Cl}_2$: Ni, 23.5; C, 19.2; H, 6.5; Cl, 28.4. Found: Ni, 24.0; C, 19.3; H, 6.6; Cl, 28.4.

$[\text{Ni}_2(\text{en})_4\text{Br}_2]\text{Br}_2$ was prepared in the same way from the corresponding bromide salts. *Anal.* Calcd for $\text{Ni}_4\text{H}_{16}\text{N}_4\text{Br}_2$: C, 14.2; H, 4.8; N, 16.55; Br, 47.2. Found: C, 14.4; H, 4.7; N, 16.7; Br, 47.2.

$[\text{Ni}_2(\text{en})_4(\text{SCN})_2]\text{I}_2$ was prepared⁹ by crystallization from an aqueous ethanolic solution (50% v/v) containing equimolar amounts of $[\text{Ni}(\text{en})_2(\text{SCN})_2]$ and NaI. The product was twice crystallized from aqueous ethanol. *Anal.* Calcd for $\text{Ni}_2\text{H}_{16}\text{N}_4\text{S}_2\text{I}_2$: Ni, 16.1; C, 16.5; H, 4.4; N, 19.25; S, 8.8. Found: Ni, 16.3; C, 16.7; H, 4.4; N, 19.4; S, 9.0.

Susceptibility measurements were made on polycrystalline samples at temperatures between 1.5 (pumped helium) and 300°K, with a null-coil pendulum magnetometer,¹⁰ using the techniques described previously.¹¹ The field dependence of the susceptibility was determined at field strengths in the range 1–15.3 kOe at several temperatures between 1.5 and 10°K.

Results

Table I contains the results of our measurements in the form of χ_A' , the field-independent susceptibility per gram atom of Ni, and also as $\mu_{\text{eff}} = 2.8273[(\chi_A' - N\alpha)T]^{1/2}$. A diamagnetic correction¹² has been included in the susceptibilities. Measurements on the thiocyanate complex were checked on three different samples; the results quoted in Table I are a typical set. From the three sets of measurements on $[\text{Ni}_2(\text{en})_4(\text{SCN})_2]\text{I}_2$, the maximum uncertainty in μ_{eff} is ± 0.05 BM; this is indicated by the error bars in Figure 4 which shows a plot of μ_{eff} and of $1/\chi_A'$ for the thiocyanate complex. The susceptibility of $[\text{Ni}_2(\text{en})_4\text{Cl}_2]\text{Cl}_2$ has been reported previously for the range 297–95°K;¹³ the present results for this range are in agreement with the reported values. The susceptibilities of all three compounds were field independent from 1 to 15.3 kOe between 1.5 and 10°K.

Discussion

The μ_{eff} vs. temperature curves for the three nickel dimers are similar. At room temperature μ_{eff} is in the range expected for octahedrally coordinated Ni(II) with a ${}^3A_2(t_{2g}^6e_g^2)$ ground state. As the temperature is lowered, μ_{eff} gradually increases until a maximum is reached in the 15–25°K temperature range. At lower

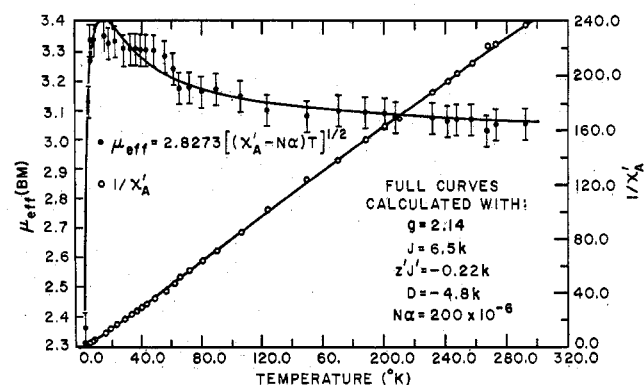


Figure 4.—Temperature dependence of μ_{eff} (BM) per Ni atom and $1/\chi_A'$ for $[\text{Ni}_2(\text{en})_4(\text{SCN})_2]\text{I}_2$.

temperatures μ_{eff} decreases rapidly. Qualitative comparison of the experimental curves, as exemplified by Figure 4, with the theoretical curves in Figure 3 indicates that there is a ferromagnetic intracuster interaction (positive J) and one or both of a much weaker antiferromagnetic interdimer interaction (negative $Z'J'$) and single-ion zero-field splitting.

Quantitative comparison of the experimental μ_{eff} with the μ_{eff} form of eq 5 and 20 leads to the results summarized in Table II. The values in the table were obtained by using a nonlinear least-squares fitting subroutine¹⁴ based on Marquardt's algorithm.¹⁵ Improved agreement between observed and calculated μ_{eff} at low temperatures is found with the four-parameter fits as compared to the three-parameter fit. The difference between the fits with positive and negative D is not significant, so that it is not possible to decide the sign of D from our measurements. The parameters D and $Z'J'$ are very strongly correlated with each other but are only weakly correlated with g and J . To illustrate this we give the parameter correlation matrix¹⁶ (Matrix I) for the fit of eq 20 with negative D to the

	MATRIX I			
	J	g	$Z'J'$	D
J	1.00	-0.77	-0.31	0.37
g	-0.77	1.00	-0.16	0.05
$Z'J'$	-0.31	-0.16	1.00	-0.96
D	0.37	0.05	-0.96	1.00

$[\text{Ni}_2(\text{en})_4(\text{SCN})_2]\text{I}_2$ data. The estimates of g and J are therefore essentially unaffected by the inclusion of zero-field splitting in the theory. Figure 4 illustrates the comparison between theory and experiment for the thiocyanate complex.

According to the above results, the increase in μ_{eff} with decreasing temperature is a consequence of the increasing population of the $S = 2$ molecular ground state. The chloride, bromide, and thiocyanate dimer molecules are almost entirely in the $S = 2$ spin state by, respectively, 14, 12, and 7°K. The combined effects of single-ion zero-field splitting and lattice antiferromagnetism causes the rapid low-temperature decrease in μ_{eff} .

In $[\text{Ni}_2(\text{en})_4\text{X}_2]\text{X}_2$ ($X = \text{Cl}, \text{Br}$) the pairs of metal

(8) H. M. State, *Inorg. Syn.*, **6**, 198 (1960).

(9) A. V. Babaeva and C. Shou-Kang, *Zh. Neorg. Khim.*, **5**, 1274 (1960).

(10) R. M. Bozorth, H. J. Williams, and D. E. Walsh, *Phys. Rev.*, **103**, 572 (1956).

(11) A. P. Ginsberg, R. C. Sherwood, and E. Koubek, *J. Inorg. Nucl. Chem.*, **29**, 353 (1967).

(12) P. W. Selwood, "Magnetochemistry," 2nd ed, Interscience, New York, N. Y., 1956, pp 78, 92.

(13) M. E. Farago, J. M. James, and V. C. G. Trew, *J. Chem. Soc.*, 728 (1967).

(14) Bell Laboratories subroutine NLLSQ by W. A. Burnette and C. S. Roberts. This is an improved version of Share Program Library SDA 3094 by D. W. Marquardt.

(15) D. W. Marquardt, *J. Soc. Ind. Appl. Math.*, **11**, 431 (1963).

(16) See the write-up accompanying Share Program Library SDA 3094 by D. W. Marquardt.

TABLE I
EXPERIMENTAL VALUES OF THE FIELD-INDEPENDENT SUSCEPTIBILITY PER NI ATOM ($\text{cm}^3 \text{G-ATOM}^{-1}$) AND OF μ_{eff} (BM) = $2.8273[(\chi_A' - N\alpha)T]^{1/2}$ WITH $N\alpha = 200 \times 10^{-6}$

Eq	Parameter	$[\text{Ni}_2(\text{en})_4\text{Cl}_2]\text{Cl}_2$										$[\text{Ni}_2(\text{en})_4\text{Br}_2]\text{Br}_2$										$[\text{Ni}_2(\text{en})_4(\text{SCN})_2]\text{I}_2$									
		Value ^a	OPL, OPU ^b	SPL, SPU ^c	Se ^d	Value ^a	OPL, OPU ^b	SPL, SPU ^c	Se ^d	Value ^a	OPL, OPU ^b	SPL, SPU ^c	Se ^d	Value ^a	OPL, OPU ^b	SPL, SPU ^c	Se ^d	Value ^a	OPL, OPU ^b	SPL, SPU ^c	Se ^d										
5	T, °K	1.52	1.57	4.21	4.30	6.3	8.25	10.1	20.6	22.3	32.6	44.5	44.7	55.0	56.5	65.5	74.0	76.5	91.0	92.0	100.0	110.0	115.0	124.0	140.0	157.0	168.5	174.5	181.5	186.5	
	$10^3\chi_A^a$	396	392	283	282	220	179	150	75.1	71.7	48.1	33.9	34.8	27.8	25.9	22.3	18.2	17.0	14.3	13.7	12.8	11.5	10.9	10.5	9.01	8.22	7.46	7.36	6.94	6.90	
	μ_{eff}	2.19	2.22	3.09	3.11	3.32	3.43	3.48	3.51	3.57	3.53	3.46	3.52	3.48	3.40	3.40	3.40	3.26	3.20	3.15	3.17	3.15	3.13	3.19	3.13	3.17	3.12	3.15	3.12	3.15	
	T, °K	192.5	196.0	204.0	206.0	208.5	223.0	226.0	227.0	231.5	238.5	239.5	246.0	258.5	267.5	294.0	296.5														
$10^3\chi_A^a$	6.53	6.30	6.27	6.05	5.62	5.56	5.67	5.42	5.31	5.38	5.10	4.84	4.85	4.28	4.35																
μ_{eff}	3.11	3.08	3.14	3.14	3.12	3.10	3.10	3.14	3.10	3.11	3.14	3.09	3.14	3.08	3.12																
20	T, °K	1.57	4.20	6.5	8.6	12.8	16.6	20.9	27.5	42.3	53.3	62.0	104.0	141.0	157.0	179.5	187.5	205.5	215.0	226.5	230.0	233.0	245.0	247.5	256.0	268.5	290.0	292.0			
	$10^3\chi_A^a$	293	259	187.5	153	109	83.6	68.5	51.9	33.8	26.1	21.8	12.1	8.75	7.85	6.84	6.61	5.97	5.81	5.41	5.39	5.29	5.06	4.94	4.84	4.59	4.21	4.23			
	μ_{eff}	1.92	2.83	3.12	3.24	3.33	3.33	3.38	3.37	3.37	3.32	3.27	3.14	3.10	3.10	3.09	3.10	3.08	3.10	3.07	3.09	3.08	3.09	3.06	3.08	3.07	3.05	3.07			
	T, °K	1.65	4.20	5.6	7.2	8.65	15.6	18.8	23.1	28.7	33.3	36.3	39.7	43.2	48.7	56.2	61.7	65.7	72.0	81.0	90.0	106.0	124.0	150.0	170.5	188.0	201.0	208.5	232.0	241.5	
$10^3\chi_A^a$	425	292	238	193	161	89.8	73.5	60.1	47.8	41.1	37.8	34.5	31.6	28.0	24.1	21.4	19.4	17.7	15.6	14.1	11.9	9.88	8.10	7.24	6.55	6.13	5.90	5.31	5.09		
μ_{eff}	2.37	3.13	3.26	3.33	3.33	3.34	3.32	3.33	3.30	3.30	3.30	3.30	3.29	3.29	3.27	3.24	3.17	3.17	3.16	3.16	3.14	3.10	3.08	3.10	3.09	3.09	3.08	3.08	3.07		
20	T, °K	248.5	258.0	267.5	273.0	292.0																									
	$10^3\chi_A^a$	4.95	4.78	4.52	4.49	4.22																									
	μ_{eff}	3.07	3.07	3.04	3.06	3.06																									

^a Diamagnetic correction $-314 \times 10^{-6} \text{ cm}^3 \text{ g-atom}^{-1}$. ^b Diamagnetic correction $-354 \times 10^{-6} \text{ cm}^3 \text{ g-atom}^{-1}$. ^c Diamagnetic correction $-367 \times 10^{-6} \text{ cm}^3 \text{ g-atom}^{-1}$.

TABLE II
RESULTS OF LEAST-SQUARES COMPARISON OF EXPERIMENTAL μ_{eff} WITH EQ 5 AND 20

Eq	Parameter	$[\text{Ni}_2(\text{en})_4\text{Cl}_2]\text{Cl}_2$				$[\text{Ni}_2(\text{en})_4\text{Br}_2]\text{Br}_2$				$[\text{Ni}_2(\text{en})_4(\text{SCN})_2]\text{I}_2$			
		Value ^a	OPL, OPU ^b	SPL, SPU ^c	Se ^d	Value ^a	OPL, OPU ^b	SPL, SPU ^c	Se ^d	Value ^a	OPL, OPU ^b	SPL, SPU ^c	Se ^d
5	J	13.8	8.8, 18.8	6.2, 21.4	0.0839	11.9	7.9, 15.9	5.7, 18.1	0.0564	7.2	6.0, 8.4	5.4, 9.0	0.0412
	g	2.14	2.10, 2.18	2.07, 2.21		2.13	2.10, 2.16	2.08, 2.18		2.14	2.12, 2.16	2.11, 2.17	
	Z'J'	-0.54	-0.62, -0.46	-0.65, -0.43		-0.80	-0.89, -0.71	-0.93, -0.67		-0.51	-0.55, -0.47	-0.57, -0.45	
	J	14.2	10.1, 18.3	7.1, 21.3	0.0638	12.4	9.9, 14.8	8.1, 16.7	0.0326	7.0	6.1, 7.9	5.4, 8.6	0.0311
20	g	2.14	2.11, 2.17	2.09, 2.19		2.12	2.10, 2.14	2.09, 2.15		2.14	2.13, 2.15	2.12, 2.16	
	Z'J'	-0.24	-0.35, -0.13	-0.40, -0.08		-0.40	-0.47, -0.33	-0.53, -0.27		-0.26	-0.31, -0.21	-0.35, 0.17	
	D(>0)	9.4	1.1, 17.9	-5.0, 24.0		9.5	4.7, 14.3	1.2, 17.8		6.8	3.4, 10.2	0.9, 12.7	
	J	15.0	11.5, 18.4	9.1, 20.9	0.0514	10.8	9.0, 12.6	7.6, 14.0	0.029	6.5	5.5, 7.5	4.9, 8.1	0.0326
20	g	2.12	2.09, 2.14	2.08, 2.16		2.12	2.10, 2.14	2.09, 2.15		2.14	2.12, 2.16	2.11, 2.17	
	Z'J'	-0.03	-0.09, 0.02	-0.17, 0.10		-0.23	-0.30, -0.16	-0.35, -0.11		-0.22	-0.28, -0.16	-0.32, -0.12	
	D(<0)	-16	-19, -13	-22, -10		-11	-14, -8	-16, -6		-4.8	-7.6, -2.0	-9.6, -0.0	

^a Least-squares best fit values of the parameters; J', Z'J', and D are given in units of k. For the fit to eq 5, the values of g and J quoted in our preliminary communication are slightly different because of the use there of a simplified version of eq 5 and, in the case of the thiocyanate complex, because of an error in the diamagnetic correction to the susceptibilities.^{1a} ^b The one-parameter lower and upper limits calculated with the value of Student's $t_{1-\alpha}(n-k)$ required for $\alpha = 0.10$. This is a one-parameter-at-a-time 90% confidence interval. ^c The support-plane lower and upper limits calculated with the variance ratio statistic $F_{1-\alpha}(k, n-k)$ required for $\alpha = 0.10$. This is a joint 90% confidence interval. ^d Se, the standard error of estimate, is a measure of the goodness of fit of the model to the data. $\text{Se} = |\Phi/(n-k)|^{1/2}$ where n is the number of data points, k is the number of parameters, and $\Phi = \sum_{i=1}^n [(\mu_{\text{eff}})_i(\text{obsd}) - (\mu_{\text{eff}})_i(\text{calcd})]^2$ is the sum of the squares of the residuals.

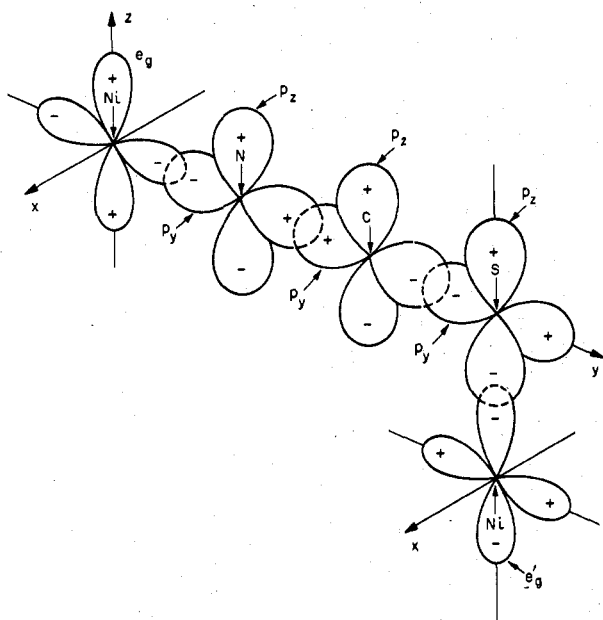


Figure 5.—Schematic illustration, in terms of atomic orbitals, of the exchange pathway $e_g || \sigma^b_y \perp \pi^b_z || e_g'$ in $[\text{Ni}_2(\text{en})_4(\text{SCN})_2]\text{I}_2$.

atoms are linked by two essentially 90° monatomic bridges. Parallel spin coupling is now well known to take place in this situation and may be understood in terms of the Goodenough-Kanamori rules¹⁷ or Anderson's expanded orbital theory.¹⁸ In terms of the latter, and using the notation $||$ to symbolize overlap and \perp to symbolize orthogonality, the pathways for parallel coupling may be written^{7a} $e_g || p_y \perp p_z || e_g'$, $e_g || p_y \perp s || e_g'$, and $e_g || s \perp p_z || e_g'$, where e_g refers to the orbitals on one metal atom and e_g' to those on the other, and s , p_y , and

p_z refer to bridge atom orbitals. These pathways, especially the first, predominate over the lone pathway for antiparallel coupling, $e_g || s || e_g'$.

In $[\text{Ni}_2(\text{en})_4(\text{SCN})_2]\text{I}_2$, where the pair of metal atoms is connected by two three-atom thiocyanate bridges, we have a more novel situation. Since the Ni-Ni distance is so great, it is clear that the exchange coupling takes place *via* the bridging thiocyanate groups. By analogy with the molecular orbital description of the isoelectronic molecule CO_2 ¹⁹ the ground state of NCS^- may be written as $(2s_N)^2(3s_S)^2(\sigma^b_s)^2(\sigma^b_y)^2(\pi^b_{x,z})^4$, where the π orbitals are of the form $\pi^b_z = c_1 2p_{zN} + c_2 2p_{zC} + c_3 3p_{zS}$ and $\pi_x = c_4 2p_{xN} - c_5 3p_{xS}$, and the σ orbitals are $\sigma^b_s = c_6 2s_C + c_7 2p_{yN} + c_8 3p_{yS}$ and $\sigma^b_y = c_9 2p_{yN} + c_{10} 2p_{yC} + c_{11} 3p_{yS}$. Assuming an idealized geometry with linear thiocyanate bridges and 90° N-Ni-S angles, the pathways for ferromagnetic coupling are $e_g || \sigma^b_y \perp \pi^b_z || e_g'$, $e_g || \sigma^b_y \perp \pi_x || e_g'$, $e_g || \sigma^b_z \perp \pi^b_z || e_g'$, and $e_g || \sigma^b_s \perp \pi_x || e_g'$. The first of these, illustrated in Figure 5, is exactly analogous to the principal pathway for ferromagnetic coupling in a monatomic 90° Ni-X-Ni bridge, namely, $e_g || p_y \perp p_z || e_g'$. The other pathways are not present in a monatomic bridge but occur here because the thiocyanate bridge is polynuclear. This description of the exchange coupling in $[\text{Ni}_2(\text{en})_4(\text{SCN})_2]\text{I}_2$ leads to the conclusion that the essential requirement for ferromagnetic coupling between metal atoms in a cluster is the availability of connecting orbitals of proper symmetry. If the connecting orbitals are multicenter molecular orbitals, the coupling can take place over long distances and through polyatomic bridges.

As a final remark we note that the decrease in J along the sequence of bridging atoms Cl^- , Br^- , NCS^- may be attributed to the increasing size of the expanded magnetic orbital and the consequent decrease in intratomic coupling on the bridging group.

(17) J. B. Goodenough, "Magnetism and the Chemical Bond," Interscience, New York, N. Y., 1963, pp 165-184.

(18) P. W. Anderson in "Magnetism," Vol. 1, G. T. Rado and H. Suhl, Ed., Academic Press, New York, N. Y., 1963, Chapter 2.

(19) For a simplified description see H. B. Gray, "Electrons and Chemical Bonding," W. A. Benjamin, New York, N. Y., 1964, pp 95-100.